Use of CFRP Overlays to Repair Fatigue Damage in Steel Plates under Tension Loading

Fatih Alemdar[1]; Regan Gangel[2]; Adolfo Matamoros, Ph.D., A.M.ASCE[3]; Caroline Bennett, Ph.D., A.M.ASCE[4]; Ron Barrett-Gonzalez, Ph.D.[5]; Stan Rolfe, Ph.D., P.E., Hon.M.ASCE[6]; and Hao Liu[7]

Abstract: Fiber-reinforced polymer (FRP) overlays have been successfully used in the aerospace industry to repair fatigue damage in aluminum plates. With this success there is potential for use of similar FRP overlays to repair fatigue damage in aging steel bridge structures. This study investigated the effectiveness of repairing fatigue damage in steel plate with adhesively bonded carbon fiber–reinforced polymer (CFRP) overlays. A total of 15 steel plate specimens with preexisting fatigue cracks were repaired with varying thicknesses of CFRP overlays to evaluate the effect of the ratio of axial stiffness of the composite to that of the underlying steel, the axial stiffness ratio (SR), on increased fatigue life and decreased applied stress. The results showed that increasing the axial stiffness ratio from 0 to 0.4 could increase the fatigue life by a factor of 10 for the most extreme conditions, and with an optimal axial stiffness ratio infinite fatigue life may be reached. Fatigue life of the steel specimens in this study was found to be dependent on both axial stiffness and applied stress range. Results from finite-element analyses validated the use of axial stiffness as a design parameter and correlated to the experimental results discussed. **DOI: 10.1061/(ASCE)CC.1943-5614.0000368.**

CE Database subject headings: Fiber reinforced polymer; Steel bridges; Rehabilitation; Tension; Fatigue.

Author keywords: CFRP; Fatigue; Steel Bridge; Repair; Retrofit.

Introduction

A significant number of aging steel bridge structures experience structural problems because of fatigue cracks. One repair technique that has been used by the Kansas Department of Transportation (KDOT) in cases in which fatigue cracks have propagated significantly into girder webs is to retrofit the web with a full-depth bolted steel splice at the location of cracking. The intent of the splice is to provide an alternate load path around the damaged web, and it is designed for the full shear demand at that web location. Attaching full-depth splice plates to the damaged web does reduce the stress in the fatigue sensitive area (Roddis and Zhao 2001); however, this is an expensive repair and there is potential that with a full-depth steel splice plate covering the damaged region of a girder, any additional crack propagation may be hidden from view and go unnoticed.

[1]Graduate Research Assistant, Univ. of Kansas, 1530 W. 15th St., Lawrence, KS 66045.

[2]Graduate Research Assistant, Univ. of Kansas, 1530 W. 15th St., Lawrence, KS 66045.

[3]Associate Professor, Univ. of Kansas, 1530 W. 15th St., Lawrence, KS 66045.

[4]Assistant Professor, Univ. of Kansas, 1530 W. 15th St., Lawrence, KS 66045 (corresponding author). E-mail: crb@ku.edu; caroline.rose.bennett@gmail.com

[5]Associate Professor, Univ. of Kansas, 1530 W. 15th St., Lawrence, KS 66045.

[6]A. P. Learned Professor, Univ. of Kansas, 1530 W. 15th St., Lawrence, KS 66045.

[7]Graduate Research Assistant, Univ. of Kansas, 1530 W. 15th St., Lawrence, KS 66045.

Note. This manuscript was submitted on June 19, 2012; approved on February 4, 2013; published online on February 6, 2013. Discussion period open until May 2, 2014; separate discussions must be submitted for individual papers. This paper is part of the ***Journal of Composites for Construction***, © ASCE, ISSN 1090-0268/04013052(10)/$25.00.

A more localized repair utilizing carbon fiber reinforced polymer (CFRP) materials could result in a more cost-effective and inspectable repair. One potential embodiment of this type of repair is a pair of CFRP overlay elements, one bonded to each face of the steel web over the crack with an epoxy resin layer. The CFRP overlays would not need to extend the full-depth of the web; instead, they could patch the region over the crack. However, before the potential of any such specific repair geometry can be effectively investigated, fundamental questions must be answered concerning the effectiveness of CFRP overlays in extending the fatigue life of steel plate loaded in tension with a preexisting fatigue crack. The aim of the research described in this paper is to provide fundamental information concerning basic proportions (thicknesses) of CFRP overlays relative to the steel to which they are bonded to effectively slow or halt fatigue crack propagation in the steel under various stress demands. The effect of bond thickness and modulus of elasticity of CFRP on the reduction in stress at critical locations was also evaluated.

Background

A significant amount of research on the use of composite materials has been carried out in the field of aerospace engineering to address fatigue problems in the fuselages of airplanes (Mall and Conley 2009; Umamaheswar and Singh 1999; Schubbe and Mall 1999a; Naboulsi and Mall 1996; Lee and Lee 2004; Liu et al. 2009b). The most recent research performed on this topic in the aerospace field has focused on the use of fiber reinforced polymer (FRP) patches to repair fatigue damage in aluminum plates. These studies have shown that FRP plates can reduce stresses in a vulnerable detail significantly if properly proportioned and bonded to the substrate. An experimental study by Mall and Conley (2009) reported that bonding a boron fiber reinforced polymer overlay to only one side of an aluminum specimen increased the fatigue crack

propagation life between four and 10 times with respect to the propagation life of an untreated specimen. Wang et al. (2002) also found an increase in fatigue crack propagation life on the order of 10 times in aluminum plates repaired with FRP patches.

In the aerospace field a commonly used parameter for proportioning composite patches for the purpose of repairing fatigue damage is the stiffness ratio:

$$\mathrm{SR} = E_{\mathrm{CFRP}} t_{\mathrm{CFRP}} / E_s t_s \quad (1)$$

where SR = stiffness ratio defined as the ratio of axial stiffness of the composite to that of the underlying steel; E_{CFRP} = modulus of elasticity of the CFRP; t_{CFRP} = thickness of the CFRP patch; E_s = modulus of the steel; and t_s = thickness of the steel plate. The SR parameter is used to determine thickness of FRP needed to repair fatigue-damaged steel plates by assuming that the driving force is redistributed in proportion to the relative axial stiffness of the two materials. For aerospace structures the recommended stiffness ratio is 1.0 (Schubbe and Mall 1999b). Schubbe and Mall (1999b) performed experimental tests on aluminum plates repaired with a bonded composite patch and found that as the stiffness ratio increased, so did the fatigue life of both thin and thick plates. Stiffness ratios of 1.0 and 1.3 were evaluated in that study.

Although the use of CFRP overlays is not widely implemented in steel structures yet, several studies have investigated their use to repair fatigue-related damage. Tavakkolizadeh and Saadatmanesh (2003) studied the effectiveness of unidirectional CFRP sheets to improve the fatigue strength of S127 × 4.5 steel girders with preexisting notch cracks. The authors reported that the fatigue-crack propagation life of the specimens with CFRP sheets was extended by a factor of approximately three compared with that of control specimens. Liu et al. (2009a) studied the tensile fatigue behavior of notched steel plates strengthened with single-ply CFRP patches. Results showed that single-sided repair extended the fatigue-crack propagation life of the specimen by a factor ranging between 2.2 and 2.7, whereas a double-sided repair extended the fatigue-crack propagation life by a factor ranging between 4.7 and 7.9. Roy et al. (2009) performed a study using the same type of materials and procedure used by Liu et al. (2009a) and showed similar increases in fatigue-crack propagation life of steel plates repaired with single-sided CFRP patches as seen in Liu et al. (2009a). Bocciarelli et al. (2009) studied the use of double-sided CFRP overlays on uncracked steel plates under fatigue loading and found that failure was precipitated by debonding of the overlays. They also found that the fatigue performance of steel plates reinforced with CFRP plates was comparable to that of steel specimens with welded steel plates.

Kaan et al. (2012) studied the behavior of uncracked plate-coverplate connections repaired with CFRP overlays. Results showed that specimen behavior, according to the AASHTO design specifications, could be improved from a fatigue design Category E' detail to fatigue design Category B' or B detail. In this study, increased fatigue crack initiation life was a direct result of maintaining adequate bond.

Analytical modeling of CFRP repairs using the finite element (FE) method is also an important technique when developing efficient retrofit schemes for steel structures. Researchers (Liu et al. 2009b; Lee and Lee 2004) have shown good agreement between the change in stress demand estimated using FE models and experimentally observed changes in fatigue-crack propagation life. In FE models that include a layer of resin between the CFRP overlay and the underlying metal, the potential for debonding can be assessed by comparing the stress demand in the resin with a limiting value. This approach was also adopted in the FE simulations conducted in this study.

Objective and Scope

The overall objective of the research described in this paper was to determine the effectiveness of CFRP overlays to repair existing fatigue damage in steel plate tested under cyclic tensile load. The scope of study included both physical and computer simulations. First, 15 steel plate specimens were repaired with CFRP overlays of various thicknesses to evaluate the effect of the axial stiffness ratio, SR, on fatigue crack propagation life and effective stress range. Second, relationships between the stiffness of the CFRP overlays and steel substrate were identified such that future CFRP repair techniques can be proportioned to effectively slow or halt fatigue crack propagation in the steel substrate. Third, the effect of bond layer thickness and CFRP overlay thickness on the reduction in hot spot stress (HSS) was evaluated using FE models. In this paper, HSS was defined as the stress at a distance half the thickness of the steel plate away from the point of peak stress, which occurred at the edge of the hole (Marquis and Kaehoenen 1995). HSS was used as an indicator of stress range, and consequently, as a measure of the effectiveness of various composite overlay configurations. This technique has been used in other companion studies aimed at examining fatigue performance and behavior of steel bridges (Hassel 2011; Kaan et al. 2012; Hartman et al. 2010). Finally, the effect of overlay stiffness on fatigue performance determined using the FE method was compared with observations from experimental results. FE simulations and experimental testing were performed on using specimens with the configuration shown in Fig 1.

Finite-Element Simulations

There are several parameters that can affect the performance of CFRP overlays as a fatigue repair technique for steel plates.

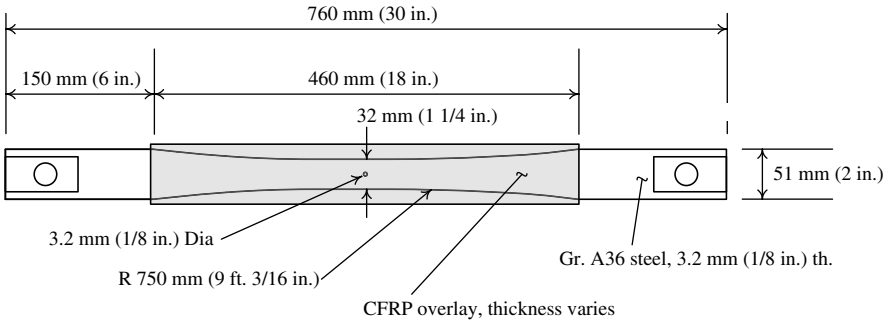

Fig. 1. Tension specimen dimensions [3.2-mm (1/8-in.) thick specimen]

A parametric study was carried out to investigate changes in the stress demand in specimens repaired with varying E_{CFRP} and t_{CFRP}. The effects of bond layer properties on peel and shear stress demands were also evaluated.

Modeling Methodology

Finite-element simulations of the specimens tested during the experimental program (Fig. 1) were carried out using the commercially-available FE analysis software *ABAQUS* version 6.8.2. The models consisted of the steel specimen with a modulus of elasticity of 200 GPa (29,000 ksi), overlaid with 6-mm (1/4-in.) thick, 458-mm (18-in.) long CFRP plates with a modulus of elasticity of 83 GPa (12,000 ksi). The CFRP overlays were attached to each side of the specimen with a 0.6-mm (25-mil) thick resin interface having a modulus of elasticity of 2 GPa (300 ksi). The study was performed by changing a single parameter while maintaining the remaining parameters constant.

FE models were developed using linear-elastic materials, and meshes were assembled using eight-node brick elements. The mesh configuration for the steel specimen part is shown in Fig. 2(a). The mesh was configured using several regions with greater mesh density near the circular opening. The mesh configuration near the opening, presented in Fig. 2(b and c), consisted of two concentric circular regions, which allowed gradually increasing element size away from the circular opening. Boundaries between the different regions of the mesh are illustrated in Fig. 2(b). A convergence study was carried out and the results are illustrated in Fig. 2(d). Because the maximum principal HSS near the circular opening was found to be insensitive to mesh size for the range of mesh densities explored, a mesh with a minimum element size of 0.25 mm (0.1 in.), shown in Fig. 2(b), was used in the study.

Interfaces between the steel, resin, and CFRP parts of the model were defined using tie constraints. Motion was restrained at one end of the model whereas the other end was free to move only in the vertical direction. Two 10.5-kN (2.35-kip) loads were applied in the vertical direction at the unrestrained end, one on each face of the model, simulating as closely as possible the manner in which the text fixture transferred the load from the testing machine. This load corresponded to a nominal testing stress range of 221 MPa (32 ksi), on the basis of the steel net section area.

It is recognized that there are studies in which FE simulations of composite repairs have been performed using nonlinear constitutive relationships. Given the objective and scope of this study, a simpler modeling approach was adopted with the goal of limiting the effect of modeling assumptions on the computational results and because the consistency between the experimental findings and simulation results did not warrant increasing the complexity of the computer simulations.

Comparisons of vulnerability to fatigue damage were performed on the basis of the maximum principal HSS as defined in the "Objective and Scope" section of this paper.

Effect of the Modulus of Elasticity of the CFRP

Six models were developed to investigate the effect of the modulus of elasticity of the CFRP, E_{CFRP}, on stress imposed on the steel specimen. E_{CFRP} was varied between 27 GPa (3,860 ksi) and 138 GPa (20,000 ksi) in increments of 28 GPa (4,000 ksi). Table 1 shows the effect of E_{CFRP} on HSS in the steel specimen. The relationship was found to be parabolic in nature and inversely proportional, indicating that there was a significant advantage associated with using an overlay, even if E_{CFRP} was relatively low. As Table 1 shows, HSS dropped by 58% with the introduction of an overlay with a very low modulus [26,600 MPa (3,860 ksi)] when compared with the unreinforced case. These data also show that increasing E_{CFRP} resulted in diminishing returns, which is important to consider when determining optimal configuration of the overlay. Increasing E_{CFRP} by a factor of five, from 26,000 MPa (3,860 ksi) to 138,000 MPa (20,000 ksi), led to a reduction in HSS by a factor of approximately three. If infinite fatigue or propagation life can be achieved with a relatively inexpensive overlay, there is no economic incentive for using stiffer, and often much more expensive, fibers.

Effect of the Thickness of the CFRP Overlay

The effect of the CFRP overlay thickness, t_{CFRP}, on HSS was evaluated by varying the CFRP overlay thickness on each side of the steel plate using values of 1.6, 2.4, 3.2, 6.4, and 12.7 mm (1/16, 3/32, 1/8, 1/4, and 1/2 in.). Results for these variations are presented in Table 2. The relationship between t_{CFRP} and maximum principal HSS was found to be inversely proportional and parabolic. The addition of the thinnest CFRP tested, 1.6 mm (1/16 in.) decreased the maximum principal HSS by a factor of two when compared with an unreinforced specimen. Similar to

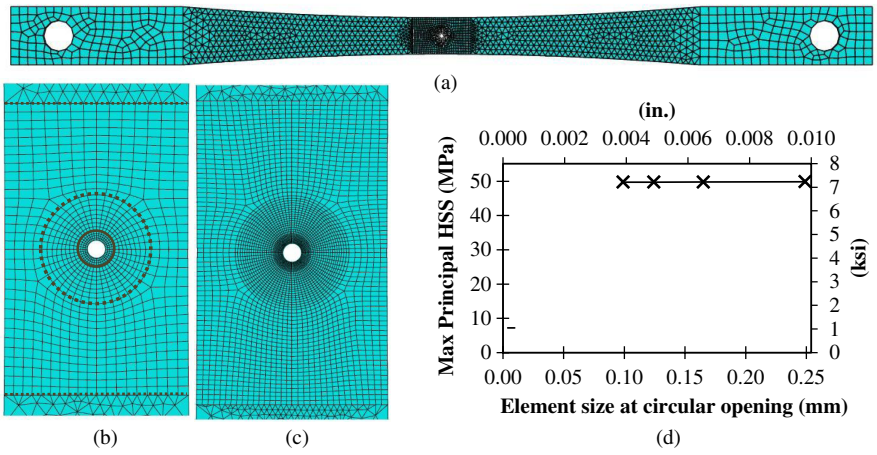

Fig. 2. (a) Finite element model mesh; (b) mesh in the vicinity of the circular opening for an element size at the opening of 0.25 mm (0.10 in.); (c) mesh in the vicinity of the circular opening for an element size at the opening of 0.12 mm (0.05 in.); (d) effect of element size at the circular opening on maximum principal HSS

Table 1. HSS versus Modulus of Elasticity of the CFRP Overlay (E_{CFRP})

E_{CFRP} MPa (ksi)	HSS MPa (ksi)
0 (0)	249 (36)
26,600 (3,860)	105 (15)
55,200 (8,000)	67 (9.7)
82,737 (12,000)	49 (7.2)
110,300 (16,000)	39 (5.7)
137,900 (20,000)	32 (4.7)

Table 2. HSS versus Thickness of the CFRP Overlays (t_{CFRP})

t_{CFRP} mm (in.)	HSS MPa (ksi)
0 (0)	249 (36)
1.6 (1/16)	126 (18)
2.4 (3/32)	99 (14)
3.2 (1/8)	85 (12.3)
6.4 (1/4)	51 (7.4)
12.7 (1/2)	28 (4.1)

the relationship when E_{CFRP} was varied, increasing t_{CFRP} exhibited diminishing returns.

Ratio of Overlay Axial Stiffness to Steel Axial Stiffness

As discussed in the "Introduction" section, one of the design parameters referenced in the literature for proportioning FRP patches is the ratio of axial stiffness of the composite patch to the axial stiffness of the underlying plate [Eq. (1)]. As Eq. (1) shows, this ratio may be modified by changing the modulus of elasticity of the FRP, thickness of the FRP, or both. The results presented in Tables 1 and 2 were used to derive two curves showing the effect of the stiffness ratio SR on the maximum principal HSS in the steel substrate (Fig. 2). For each curve, one of the two parameters (E_{CFRP} or t_{CFRP}) was varied while maintaining the other constant. All other parameters were equivalent to that of the base model.

The results presented in Fig. 3 show that changing SR by changing E_{CFRP} had similar results than changing SR by altering t_{CFRP}. There was a common trend, in that sequential increments in E_{CFRP} and t_{CFRP} resulted in similar reductions of HSS. Therefore, how the axial stiffness parameter was changed did not significantly affect the magnitude of the stress reduction.

The parameter that did have a significant effect on the HSS demand was the SR. Using an SR of approximately 0.41 decreased the maximum principal HSS by a factor of two, when compared with the stress demand in an unreinforced specimen. Increasing the SR of the overlay by a factor of eight to approximately 3.3 had a much smaller effect, decreasing the maximum principal HSS by a factor of five. The results in Fig. 3 confirm that the effect of the stiffness ratio on HSS decreased with increasing in stiffness ratio, and that the reduction in HSS had dropped significantly at an SR of 1.0. For these specimens, modeled with a 221 MPa (32 ksi) testing stress range, it is the opinion of the authors increasing SR of the overlay beyond 1.0 has limited benefits.

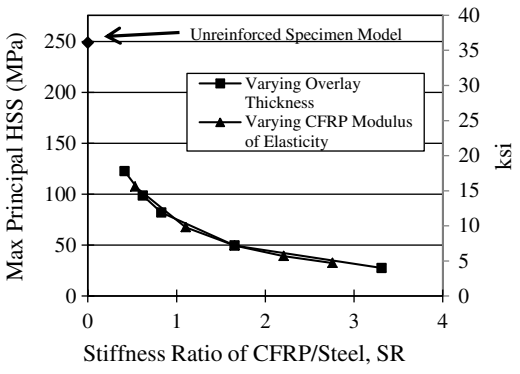

Fig. 3. Effect of stiffness ratio on maximum principal Hot Spot Stress in the steel

Effect of Thickness of Bond Layer

One of the parameters often neglected in FE simulations of retrofit measures with composite overlays is the flexibility inherent to the adhesive resin used to bond the overlay to the metal substrate. It has often been assumed that the thickness of such a layer is very small, and that there is perfect bond between the composite and the substrate (Sabelkin et al. 2006; Liu et al. 2009b; Mall and Conley 2009). Explicit modeling of this layer provides an indication of the average shear demand on the resin and the tensile demand on the resin-steel interface, which can be used to gauge the potential for debonding. Because the shear and tensile demands on the resin are affected by the thickness of the resin layer, this is an important parameter to consider in terms of fatigue and fatigue-crack propagation life.

Five different models were developed to investigate the effect of the thickness of the interface bond layer, t_{resin}, between the CFRP overlay and the steel substrate. The interface layer thickness was varied from 0.6 mm (20 mils) to 5 mm (200 mils). Results discussed by Alemdar (2011) found that the maximum principal HSS was not significantly affected by t_{resin}. However, another important design consideration is the effect of t_{resin} on the stress demand at the resin layer itself. This is important because maintaining a bond between the composite and the steel is critical to the successful performance of the retrofit scheme, and higher stress demands increase the probability of fatigue failure at the interface. Fig. 4 shows the stress demand along the resin layer for a model with $t_{resin} = 0.6$ mm (20 mil). A closed-form solution for a plate with constant width and without a circular hole presented by Bocciarelli et al. (2009) is also included for reference. Fig. 4 shows that as expected based from the closed-form solution, the shear and peel stresses (out-of-plane stress) were relatively low along most of the interface. Stress demands were greatest at the ends of the interface, which is the location considered to be the most susceptible to failure.

Fig. 5 presents the variation of peak shear and peel stresses as a function of the t_{resin}. Also, Fig. 5 has the closed-form solution presented by Bocciarelli et al. (2009). The results show that increasing

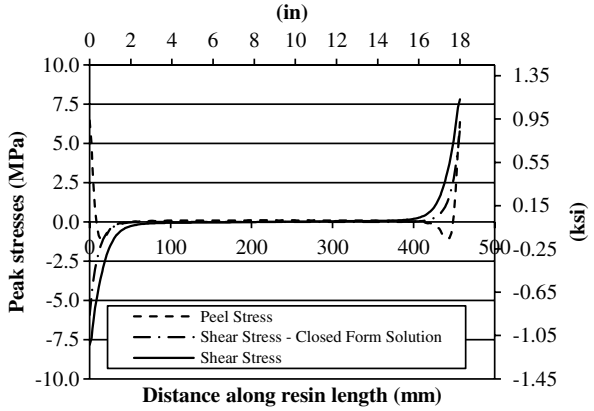

Fig. 4. Peak stresses along CFRP overlay on resin layer end of hole

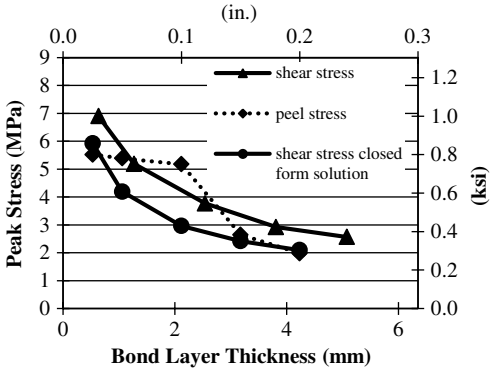

Fig. 5. Peak stresses demand on CFRP layer as a function of resin layer thickness

t_{resin} from 0.6 mm (20 mil) to 5.0 mm (200 mil) caused a reduction in peak shear demand by approximately 66%. Fig. 5 also shows that the same increase in t_{resin} led to a reduction in peak peel stresses by approximately 50%. The trend observed for the peel stress was different from that observed for the shear stress in that the peel stress demand was relatively insensitive to t_{resin} for thicknesses less than 2.5 mm (100 mil), with a significant reduction in stress for t_{resin} greater than that. These data show that although the thickness of the interface layer may not be relevant to fatigue-crack propagation life because of the negligible effect on the stress range, it is a very important parameter in terms of the bond performance of the interface layer under cyclic loading.

Experimental Program

The primary goal of the experimental program was to evaluate the effect of the stiffness ratio on fatigue-crack propagation life of steel specimens with preexisting fatigue cracks repaired using CFRP overlays. Fatigue cracks were propagated on each side of the drilled and reamed hole at the center of the specimen, shown in Fig. 1, until either of the cracks reached a length of approximately 7 mm (0.3 in.). After the initial crack length of 7 mm (0.3 in.) was reached, each specimen was repaired using CFRP overlays. Fifteen specimens were tested, shown in Table 3.

Of the four parameters in Eq. (1) that could have been varied to alter the stiffness ratio, two were varied in this study: t_{CFRP} and the thickness of the steel plate, t_s. Testing was conducted at stress ranges of 166 MPa (24 ksi), 221 MPa (32 ksi), and 263 MPa (38 ksi), to evaluate effect of SR at various stress ranges.

Measured material properties are presented in Tables 4 and 5. Coupon tests (ASTM 2008) from single-layered specimens showed that E_{CFRP} was approximately 83 GPa (12,000 ksi). Liu et al. (2009a) observed in their experiments that after the second layer of CFRP the strain demand quickly dropped; therefore, E_{CFRP} used for the computer simulations was selected to be between measured values for one and three layers. The modulus of elasticity of the 9412 Hysol resin (Henkel Corporation, Rocky Hill, Connecticut), E_{resin}, was also measured using coupon tests (Table 5) performed as prescribed by ASTM (2008). The measured E_{resin} was 2.1 GPa (300 ksi).

Table 3. Specimen Test Matrix and Results

Specimen designation	Specimen thickness mm (in.)	CFRP overlay thickness mm (in.)	Stress range MPa (ksi)	Fatigue crack propagation life
F15	3 (1/8)	1.6 (1/16)	263 (38)	18,900
F3	3 (1/8)	1.6 (1/16)	221 (32)	60,000
F6	3 (1/8)	1.6 (1/16)	166 (24)	340,700
Pick12	3 (1/8)	2.4 (3/32)	221 (32)	271,100
Pick11	3 (1/8)	3.2 (1/8)	263 (38)	95,100
F14	3 (1/8)	3.2 (1/8)	221 (32)	313,050
F2	3 (1/8)	3.2 (1/8)	166 (24)	1,450,095
Pick10	3 (1/8)	6.4 (1/4)	263 (38)	282,550
Pick13	3 (1/8)	6.4 (1/4)	221 (32)	Run-out
Pick7	3 (1/8)	6.4 (1/4)	166 (24)	Run-out
F27	3 (1/8)	12.8 (1/2)	221 (32)	Run-out
F4-25	6 (1/4)	1.6 (1/16)	221 (32)	15,600
F4-21	6 (1/4)	3.2 (1/8)	221 (32)	160,150
F4-23	6 (1/4)	6.4 (1/4)	221 (32)	571,650
F4-20	6 (1/4)	12.8 (1/2)	221 (32)	Run-out

Steel Specimen Dimensions

The specimens were fabricated using grade A36 steel and were either 3-mm (1/8-in.) or 6-mm (1/4-in.) thick. For specimens with a thickness of 3 mm (1/8 in.), the measured average yield strength was 319 MPa (46 ksi), and the measured tensile strength was 381 MPa (55 ksi). For specimens with a thickness of 6 mm (1/4 in.), the measured average yield strength was 335 MPa (48 ksi), and the measured tensile strength was 495 MPa (72 ksi) (Crain 2010).

Specimen dimensions for 3-mm (1/8-in.) thick specimens are shown in Fig. 1. There were three dimensions changed for 6-mm (1/4-in.) thick specimens with respect to those shown in Fig. 1. First, the width at each end was 63.5 mm (2.5 in.) instead of 60.8 mm (2.0 in.). Second, the width at the reduced net section was 44.5 mm (1.75 in.) instead of 31.8 mm (1.25 in.). Third, the diameter of the drilled and reamed hole at the specimen center was equal to the thickness of the specimen, 6 mm (1/4 in.).

Fabrication and Attachment of the Multilayered CFRP Overlays

The multilayered CFRP overlays were prefabricated and subsequently attached to the steel specimens. Step-by-step instructions, photographs, and diagrams illustrating the fabrication process are presented by Alemdar (2011) and Gangel (2012). Each CFRP overlay consisted of multiple layers of bidirectional preimpregnated carbon fiber plies. Scotch-Weld Epoxy adhesive (1838 B/A Green) (Industrial Adhesives and Tapes Division, St. Paul, Minnesota) was used between certain layers to ensure that there was a sufficient amount of resin to prevent voids from occurring during the curing process. Table 6 summarizes the number of

Table 4. Measured Material Properties for Continuous CFRP

Number of layers in coupon	Number of coupons	Average modulus of elasticity GPa (ksi)	Standard deviation GPa (ksi)
1	3	85.8 (12,440)	10.0 (1,450)
3	4	75.3 (10,930)	10.9 (1,580)
5	3	61.7 (8,940)	0.3 (42.0)

Table 5. Measured Material Properties for 9412 Hysol Resin

Coupon thickness mm (in.)	Number of coupons	Average modulus of elasticity GPa (ksi)	Standard deviation GPa (ksi)
6 (1/4)	6	2.1 (303)	0.2 (25)

Table 6. Fabrication of Multilayered CFRP Overlays

Overlay thickness mm (in.)	Single carbon fiber plies	Scotch weld epoxy adhesive	Placement of adhesive
1.6 (1/16)	2	1	After 1st ply
2.4 (3/32)	3	1	After 2rd ply
3.2 (1/8)	4	2	After 2rd ply
6.4 (1/4)	8	3	After 3rd and 5th ply
12.8 (1/2)	16	4	After 4th, 8th, and 12th ply

carbon fiber plies and Scotch Weld Epoxy adhesive layers used in each CFRP overlay.

The overlays were fabricated using a mold consisting of aluminum plates placed between bolted steel plates. Preimpregnated carbon fiber plies were cut to dimensions of approximately 457 × 152 mm (18 × 6 in.), which was double the size of the overlays. CFRP sheets were placed on the bottom steel plate of the mold, and were added one layer at a time. A single sheet of Scotch-Weld Epoxy adhesive (1838 B/A Green) (Industrial Adhesives and Tapes Division, St. Paul, Minnesota) resin with the same dimensions was added, following the schedule presented in Table 6. The overlay was surrounded by an aluminum spacer with a thickness equal to that of the desired overlay thickness. The top steel plate of the mold was then placed on top of the CFRP stack, and pressure was applied by tightening the bolts around the perimeter of the mold to reach the target thickness. Then, the overlay was placed in a curing oven preheated to a temperature of 175°C (347°F). Overlays were cured inside the mold for three hours, and subsequently allowed to cure at room temperature for 48 hours. After the curing process was completed, the CFRP overlays were taken out of the metal molds and cut to final dimensions of 457 × 64 mm (18 × 2.5 in.) using a diamond saw. Sand paper (grade 400) was used to smooth the edges of the CFRP overlays.

To develop adequate bond, the steel surface was prepared by a process of abrading and cleaning. Abrading consisted of roughening of the surface with a hand grinder to achieve a surface roughness of approximately 0.8 mm (30 mils). After abrading, cleaning of the surface was performed using acetone and methanol. Overlays were attached to the steel specimens using Hysol 9412 epoxy resin (Henkel Corporation, Rocky Hill, Connecticut), which has a nominal shear strength of 28 MPa (4 ksi). The thickness of the Hysol layer was 0.6 mm (24 mil), maintained during fabrication by using six spacers evenly distributed throughout the interface. Drafting tape surrounding the steel plate was used to prevent leaking of the Hysol resin, and pressure was applied to maintain $t_{\text{resin}} =$ 0.6 mm (24 mils). After two days of room-temperature curing the interface bond layer, the specimen was cleaned of remnant resin using a chisel and a heat gun.

Test Procedure

A cyclic tensile load was applied at the ends of the specimen using an MTS closed-loop servo-controlled loading system. The stress range applied to the steel specimen, $\Delta\sigma_{st}$, was determined on the basis of the following equation:

$$\Delta\sigma_{st} = \frac{F_{\text{actuator}}}{A_{\text{net},st}} \tag{2}$$

where F_{actuator} = force or load recorded by the actuator and $A_{\text{net},st}$ = nominal net cross sectional area of the steel at the reduced cross-section less the area of the drilled hole. These values, although not representative of the peak stress demand, were adopted to simplify the comparison between various specimens. The ratio of minimum to maximum stress was maintained constant at $R = 0.1$. The rate of fatigue-crack propagation was evaluated at three different stress ranges, 262 MPa (38 ksi), 221 MPa (32 ksi), and 166 MPa (24 ksi).

The propagation life of the steel specimens used in this study was calculated for different stress range demands on the basis of established theoretical expressions. Theoretical crack lengths at a given number of cycles were determined using the following equation presented by Barsom and Rolfe (1999):

$$\frac{da}{dN} = A(\Delta K)^m \tag{3}$$

where A and m = properties constant for a material; ΔK = stress intensity factor range; a = crack length; and da = change in crack length. Material constants of $A = 3.6 \times 10^{-10}$ and $m = 3$ were adopted, which correspond to values for ferrite-pearlite steel (Barsom and Rolfe 1999). Because fatigue cracks extended from a round hole on a plate with a finite width, ΔK was calculated using the following equation (Barsom and Rolfe 1999):

$$\Delta K = \Delta\sigma\sqrt{\frac{\pi \times a_{\text{avg}}}{Q}} \times f\left(\frac{a}{r}\right) xf\left(\frac{a}{b}\right) \tag{4}$$

where $\Delta\sigma$ = applied testing stress range; a_{avg} = average crack length between incremental calculation steps; Q = flaw-shape parameter (measured as 1.0 in this case); $f(a/r)$ = function of the radius of the drilled hole to crack length; and $f(a/b)$ = function of the crack length to finite width of the tensile specimen. Alemdar (2011) showed that good agreement was found between the calculated and measured crack progressions for unretrofitted specimens shown in Eqs. (3) and (4).

A comparison between observed fatigue-crack propagation rate of the specimens with CFRP overlays and the calculated fatigue-crack propagation rate in unreinforced specimens with low stress demands is presented in Fig. 6. As shown in Fig. 6, the crack propagation rate of a specimen repaired with CFRP overlays subjected to a stress range of 166 MPa (24 ksi) was similar to that of an unrepaired specimen subjected to a stress range of 35 MPa (5 ksi) on the basis of theoretical values. These results indicate that the presence of the overlay resulted in a reduction of approximately 80% in the stress range. The test of the specimen repaired with multilayered CFRP overlay subjected to a stress range of 166 MPa (24 ksi)

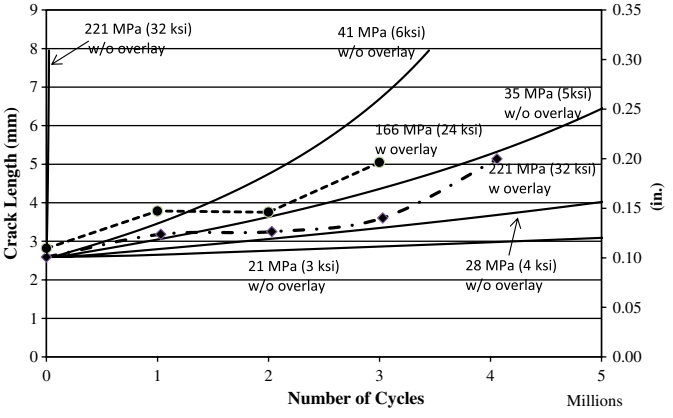

Fig. 6. Crack progression in 3-mm (1/8-in.) thick specimens; solid lines are added for comparison and correspond to theoretical crack progressions calculated using Eq. (4) with material constants of $A = 3.6 \times 10^{-10}$ and $m = 3$ for various stress ranges in a specimen configuration without overlays

was stopped after 4 million cycles, after crack growth started to become noticeable. Had the fatigue crack in this specimen continued to propagate at the theoretical rate for an unreinforced specimen under a stress range of 35 MPa (5 ksi), it would have reached a crack length of 7.6 mm (0.3 in.) at approximately 6 million cycles. A similarly loaded unrepaired steel specimen reached a crack length of 7.6 mm (0.3 in.) at only 50,000 cycles (Alemdar 2011).

Testing of the remaining specimens with CFRP overlays was carried out without removing the overlays for inspection so that that any cumulative damage to the interface layer and the composite overlay could be directly accounted for in the test results. Each test was terminated after the specimens reached failure or run-out. Failure of these specimens was defined as fatigue-crack propagation completely through the width of the steel specimen; however, crack propagation and failure could not be tracked visually because of the bonded overlays. Instead, failure was indicated by a decrease in the percent change in stiffness of the system. The percent change in stiffness was calculated using the following equation:

$$\%\text{change in } K = [(\delta L/\delta P) - K_{\max}]/K_{\max} \quad (5)$$

where K = stiffness of the combined steel and CFRP overlays; δL = change in load placed on the specimen; δP = change in position from the testing machine; and $K_{\max}$ = maximum stiffness recorded during testing. Run-out was defined as exceeding the AASHTO S-N curve for a Category A detail at the corresponding nominal stress range (AASHTO 2010).

The relationship between the change in stiffness and the number of cycles for 6-mm (1/4-in.) thick specimens tested at 221 MPa (32 ksi) are presented in Fig. 7. The relationship between the stiffness and the number of cycles for all the specimens tested in the study is reported by Gangel (2012) and Alemdar (2011).

Experimental Results

The fatigue-crack propagation life of the steel substrate from an initial crack length of 7.6 mm (0.3 in.) to complete failure in the steel was determined on the basis of the monitored change in stiffness calculated using Eq. (5). For all specimens a significant increase in compliance was observed at a given number of cycles during testing (Fig. 7). Because testing was performed under load control, any increase in compliance had to be caused by softening of the specimens, which is indicative of damage. An increase in compliance could be caused by loss of bond, damage in the composite overlays, or a reduction in the net cross sectional area of the steel specimen. Because neither the composite overlays nor the interface layer showed signs of damage or distress, it was hypothesized that gradual increases in compliance were caused primarily by the reduction of the net cross sectional area of the steel specimen. Propagation of the fatigue crack through the entire cross section of the specimen led to 100% of the load being transferred through the composite overlays. This new load path caused a rapid increase in the damage to the overlays in the vicinity of the fatigue crack and to local loss of bond, leading to a large increase in compliance. The number of cycles at which a sudden and significant change in compliance was observed was adopted as the fatigue propagation life for the specimen. On the conclusion of testing, the CFRP overlays were removed to inspect the steel specimen and confirm that the fatigue crack had in fact propagated through the entire net section of the steel. The number cycles to failure for each specimen determined in this manner are summarized in Table 3 and Fig. 8(a and b).

For specimens Pick 13, Pick 7, F27, and F4-20, a significant change in compliance was never observed and these specimens were classified as run-out. The stress reduction in the steel because of the alternate load path provided by the CFRP overlay was sufficient to drive the demand below the fatigue-crack propagation threshold (Barsom and Rolfe 1999). The composite overlays were removed for inspection after testing was complete, and it was confirmed that the fatigue cracks had not propagated fully through the steel cross-sections.

Effect of Stiffness Ratio

The fatigue-crack propagation lives determined previously were compared on the basis of the axial stiffness ratio. The value of SR was determined for each specimen on the basis of $E_{\text{CFRP}} =$ 83 GPa (12,000 ksi); the measured thickness of the steel, t_s; the CFRP overlay thickness used, t_{CFRP}; and the modulus of elasticity of steel, E_s (200 GPa, 29,000 ksi). Fig. 9 shows the fatigue-crack propagation life of each specimen versus the stiffness ratio, SR. For specimens that reached run-out (the last point of each curve, outside

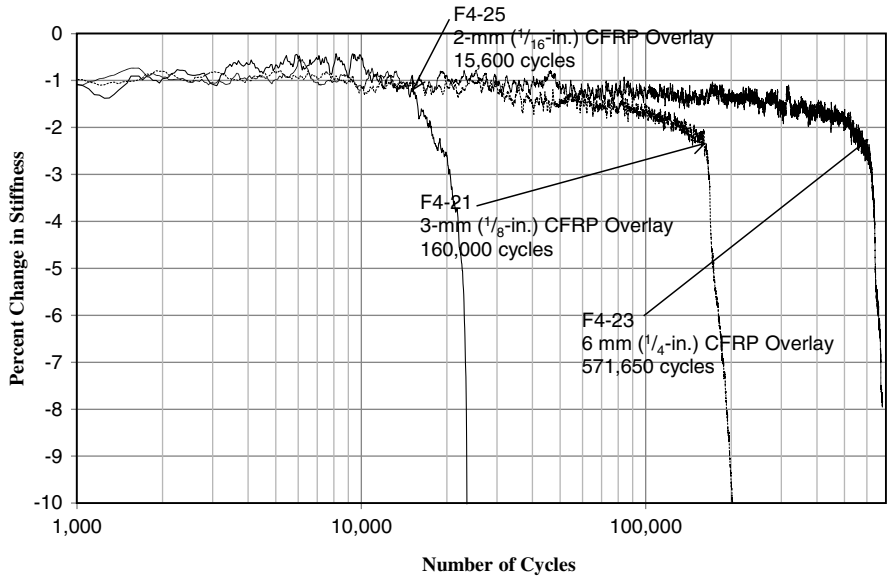

Fig. 7. Percent change in stiffness of 6-mm (1/4-in.) thick specimens tested at 221 MPa (32 ksi)

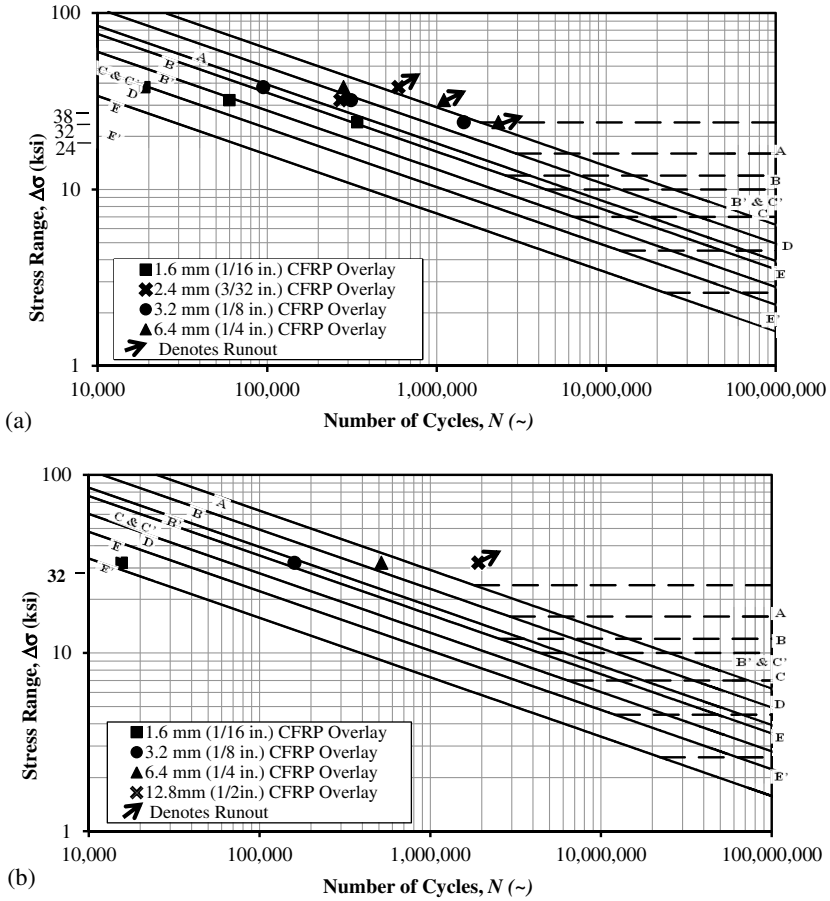

Fig. 8. S-N diagram for propagation life: (a) 3-mm (1/8-in.) thick specimens; (b) 6-mm (1/4-in.) thick specimens

the range of the graph), the number of cycles to failure was extrapolated using accepted models of theoretical crack propagation presented by Barsom and Rolfe (1999). Extrapolated points (not shown) for the four curves were 22.9, 6.8, 3.9, and 3.2 million cycles, corresponding to SR values of 1.66, 1.66, 1.66, and 3.2, respectively.

Fig. 9 shows that the effect of the SR was dependent on the applied stress range. For a specific stiffness ratio, as the stress range increased the fatigue life decreased, as expected. However, this trend was not proportional. Much greater improvement was observed when the stress range decreased from 221 MPa (32 ksi) to 166 MPa (24 ksi) than when the stress range decreased from 263 MPa (38 ksi) to 221 MPa (32 ksi).

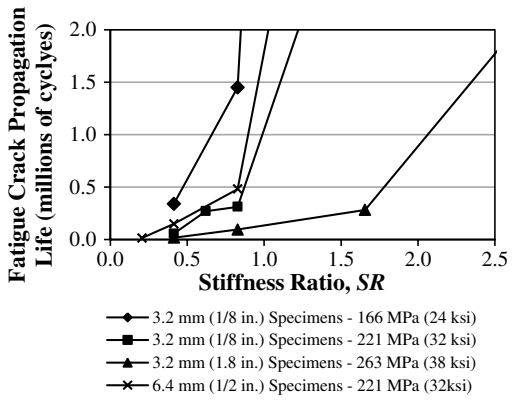

Fig. 9. Fatigue-crack propagation life for all specimens treated with CFRP overlays and an initial crack length of 7 mm (0.3 in.)

Fig. 9 also shows a relationship between propagation life and SR that may be approximated as bilinear. For all specimens, the fatigue-crack propagation life increased as the stiffness ratio increased. For each stress range there was a stiffness ratio at which the slope of the curve had a sudden increase, trending towards infinity. Past this point, small increases in the stiffness ratio resulted in propagation lives that vastly exceeded run-out. It is clear from Fig. 9 that the critical SR at which each set of data trended towards infinity increased with stress range. The critical SR for specimens tested at stress ranges of 166 MPa (24 ksi), 221 MPa (32 ksi), and 263 MPa (38 ksi) ksi were approximately 0.8, 1.0, and 1.6, respectively, regardless of specimen thickness. These results indicate that as stress range increases, the stiffness ratio must be increased to achieve infinite fatigue life.

Because the critical width of the 6-mm (1/4-in.) thick specimens differed from that of the 3-mm (1/8-in.) thick specimens, failure of the former specimens was as assumed to be the number of cycles at which the crack reached a length of 14 mm (9/16 in.). Therefore, the propagation life used in the comparisons corresponds to the same crack growth for all specimens, regardless of specimen thickness, allowing a direct comparison between the two. A direct comparison between the 3-mm (1/8-in.) thick and the 6-mm (1/4-in.) thick specimens tested at 221 MPa (32 ksi) (Fig. 9) shows that, for the same stiffness ratio, the thicker specimen had the greater propagation life. However, both specimens had approximately the same critical stiffness ratio.

Given the relatively large initial crack size of 7.6 mm (0.3 in.) relative to the remaining steel net section, control specimens were

Table 7. Theoretical Fatigue Life of Un-retrofitted Specimen and Comparative Increase in Fatigue Life of CFRP-repaired Specimens

		3-mm (1/8-in.) steel specimens			6-mm (1/4-in.) steel specimens		
		Stress range			Stress range		
Description	Stiffness ratio	166 MPa (24 ksi)	221 MPa (32 ksi)	263 MPa (38 ksi)	166 MPa (24 ksi)	221 MPa (32 ksi)	263 MPa (38 ksi)
Theoretical fatigue crack propagation life (cycles) caclulated using Eqs. (3) and (4)	0	6,891	2,907	1,736	10,423	4,397	2,625
Increase in fatigue life from theoretical values to measured values	0.21	—	—	—	—	3	—
	0.41	49.4	19.2	10.9	—	34	—
	0.62	—	93.3	—	—	—	—
	0.83	210.4	107.7	54.8	—	109.5	—
	1.66	Run-out	Run-out	162.8	—	Run-out	—
	3.31	—	—	Run-out	—	—	—

not tested in this study as their fatigue lives would have been quite low in the unreinforced condition. However, theoretical crack propagation lives for unretrofitted specimens were determined using Eq. (3). With the calculation of ΔK from Eq. (4), the theoretical number of cycles to failure of an unretrofitted specimen can be found from Eq. (3) if the change in crack length (da) is set as the distance from an initial crack length of 7.6 mm (0.3 in.) to the edge of the specimen. The results of this theoretical fatigue-crack propagation life for un-retrofitted specimens are shown in Table 7 designated as having a stiffness ratio of zero.

After the theoretical fatigue-crack propagation life of unretrofitted specimens was calculated for an initial crack length of 7.6 mm (0.3 in.), it was compared with the fatigue-crack propagation lives of CFRP repaired specimens, which are presented in Table 3. The ratio of observed fatigue-crack propagation life of the various retrofitted specimens to calculated fatigue life of the unretrofitted specimen is presented in Table 7. Table 7 shows that the applied stress range played a crucial role in the level of fatigue life improvement that was achieved through use of CFRP overlays. When the stress range decreased 16%, from 263 MPa (38 ksi) to 221 (32 ksi), the ratio of increase in fatigue-crack propagation life was approximately doubled for stiffness ratios of 0.41 and 0.83. The same held true when the applied stress range was decreased from 221 MPa (32 ksi) to 166 MPa (24 ksi). Although this means that a CFRP overlay repair was more effective at a lower stress range, the improvements observed at very high stress ranges are still promising. For a specimen with a thickness of 6 mm (1/4 in.) tested at a stress range of 221 MPa (32 ksi), the smallest stiffness ratio tested (0.21) the fatigue propagation life increased by a factor of three when compared with the theoretical fatigue-crack propagation life of an unretrofitted specimen. At 263 MPa (38 ksi) and a stiffness ratio of 0.41, the fatigue life of the specimen with the same thickness increased by a factor of 10.9. For specimens with a thickness of 3 mm (1/8 in.), increasing the stiffness ratio to 1.66 at 263 MPa (38 ksi) increased the fatigue life by a factor of 162, when compared with that of an unretrofitted specimen.

Drastic increases in fatigue-crack propagation life can be attributed to the reduced applied stress imposed on the steel. The stress ranges corresponding to the fatigue-crack propagation lives presented in Table 3 were determined using the relationships from Eqs. (3) and (4). For example, specimen F15 was tested at a stress range of 263 MPa (38 ksi) on the basis of the measured cross-section of the steel; however, the experimental fatigue-crack propagation life presented in Table 3 corresponds to an effective applied stress range of approximately 118 MPa (17 ksi) on the basis of the measured cross-section of the steel. Fig. 10 presents the effective stress ranges for all steel tensile specimens on the basis of their calculated stiffness ratio. The reductions in stress follow the same patterns determined during the FE analysis and is shown in Fig. 3. Figs. 3 and 10 show a relationship between the stiffness ratio and stress reduction that is parabolic and inversely related in nature.

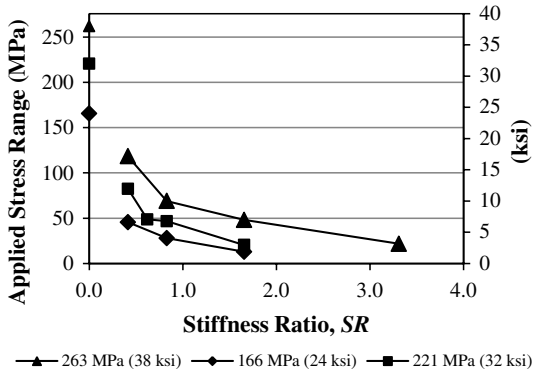

Fig. 10. Equivalent applied stress of all specimens treated with CFRP overlays and an initial crack length of 7 mm (0.3 in.)

Specimen Debond Behavior

Of the 15 specimens tested with initial crack lengths of 0.3 in., only one specimen, F4-20, experienced partial debonding between the steel and CFRP overlays. This specimen represented the thickest steel plate tested, combined with the thickest CFRP overlay tested. This suggests that the combination of very thick components led to independent behavior in terms of deformation, instead of system deformation. It is hypothesized that this behavior resulted in fatigue-crack initiation in the resin layer at the bottom and top of the CFRP overlay, and subsequent crack propagation towards the center of the length of the overlay. The fatigue crack in the bond layer was noticed at a length of approximately 38 mm (1.5 in.). At this point, a steel collar consisting of two steel plates bolted around each end of the specimen was attached to prevent further debonding (Gangel 2012). The debonding never approached the region of the fatigue crack in the steel because it was arrested with the steel collar installation; therefore, the results from this specimen are presented as comparable to the others in the study.

Conclusions

Results of an experimental and analytical study examining the use of CFRP overlays to repair fatigue cracks in steel plates has resulted in the following conclusions:

- Experimental results showed that as stress range was increased, a greater stiffness ratio was required for the fatigue-crack propagation life to tend towards infinity. At 166 MPa (24 ksi), 221 MPa (32 ksi), and 263 MPa (38 ksi) the number of cycles to failure tended towards infinity at stiffness ratios of 0.8, 1.0, and 1.6, respectively.
- Both FE analysis and experimental results showed a diminishing effect on stress demand as the stiffness ratio increased. On the basis of these results it is the opinion of the authors that the greatest benefit of using overlays to reduce the stress demand is achieved for stiffness ratios below unity.
- Experimental results showed that bonding of prefabricated multilayered CFRP overlays increased the theoretical fatigue-crack propagation life of unretrofitted steel specimens by at least three times and up to 162 times before experimental specimens reached run-out.
- The observed increase in fatigue-crack propagation life matched or was significantly higher than values ranging between 3 and 10 reported in previous studies on aluminum plates, steel plates, and steel beams. The main difference between the overlays used in this study and those used in other studies is that the stiffness ratio SR was significantly higher in this study than identified in previous literature.

Implications of the fundamental research described in this paper are significant. Research presented within this paper has shown that use of CFRP overlays to repair cracks in steel members can be a highly effective means of reducing the stress demand and greatly prolonging the fatigue-crack propagation life of steel substrate. This work has provided a basis for proportioning CFRP overlays for effectiveness in halting/slowing fatigue-crack propagation, based on nominal stress range and the stiffness ratio between the overlay and the steel.

Future research is advised to better understand the demands on and the behavior of CFRP overlays bonded to steel substrate. Topics that should be studied include testing thicker steel plates representative of bridge girder webs and investigating wide steel plates with a bonded overlay element of lesser width.

References

AASHTO. (2010). *LRFD bridge design specifications*, 5th Ed., Washington, DC.

ABAQUS 6.8.2 [Computer software]. Providence, RI, Dassault Systèmes.

Alemdar, F. (2011). "Repair of bridge steel girders damaged by distortion-induced fatigue." Ph.D. thesis, Dept. of Civil, Architectural, and Environmental Engineering, Univ. of Kansas, Lawrence, KS.

ASTM. (2008). "Standard test method for tensile properties of polymer matrix composite materials." *ASTM D3039/D3039M-08*, West Conshohocken, PA.

Barsom, J. M., and Rolfe, S. T. (1999). "Fatigue and fracture behavior of welded components." *Fracture and Fatigue Control in Structures*, 3rd Ed., ASTM, West Conshohocken, PA, 35–53.

Bocciarelli, M., Colombi, P., Fava, G., and Poggi, C. (2009). "Fatigue performance of tensile steel members strengthened with CFRP plates." *Compos. Struct.*, 87(4), 334–343.

Crain, J. (2010). "Fatigue enhancement of undersized, drilled crack-stop holes." M.S. thesis, Dept. of Civil, Architectural, and Environmental Engineering, Univ. of Kansas, Lawrence, KS.

Gangel, R., (2012). "Use of CFRP overlays to repair fatigue damage in steel bridge girders and components." M.S. Thesis, Dept. of Civil, Architectural, and Environmental Engineering, Univ. of Kansas, Lawrence, KS.

Hartman, A., Hassel, H., Adams, C., Bennett, C., Matamoros, A., and Rolfe, S. (2010). "Effects of lateral bracing placement and skew on distortion-induced fatigue in steel bridges." *Transportation Research Record No. 2200*, Transportation Research Board, 62–68.

Hassel, H. L. (2011). "An analytical evaluation of distortion-induced fatigue in steel bridges." M.S. thesis, Dept. of Civil, Architectural, and Environmental Engineering, Univ. of Kansas, Lawrence, KS.

Kaan, B. N., Alemdar, F., Bennett, C. R., Matamoros, A., Barrett-Gonzalez, R., and Rolfe, S. (2012). "Fatigue enhancement of welded details in steel bridges using CFRP overlay elements." *J. Compos. Constr.*, 10.1061/(ASCE)CC.1943-5614.0000249, 138–149.

Lee, W. Y., and Lee, J. J. (2004). "Successive 3D FE analysis technique for characterization of fatigue crack growth behavior in composite-repaired aluminum plate." *Compos. Struct.*, 66(1–4), 513–520.

Liu, H. B., Al-Mahaidi, R., and Zhao, X. L. (2009a). "Experimental study of fatigue crack growth behaviour in adhesively reinforced steel structures." *Compos. Struct.*, 90(1), 12–20.

Liu, H. B., Xiao, Z. G., Zhao, X. L., and Al-Mahaidi, R. (2009b). "Prediction of fatigue life for CFRP-strengthened steel plates." *Thin-Walled Struct.*, 47(10), 1069–1077.

Mall, S., and Conley, D. S. (2009). "Modeling and validation of composite patch repair to cracked thick and thin metallic panels." *Compos., Part A*, 40(9), 1331–1339.

Marquis, G., and Kahonen, A. (1995). "Fatigue testing and analysis using the hot spot method." *VTT Publication 239* , Technical Research Centre of Finland, 37.

Naboulsi, S., and Mall, S. (1996). "Modeling of a cracked metallic structure with bonded composite patch using the three layer technique." *Compos. Struct.*, 35(3), 295–308.

Roddis, W. M., and Zhao, Y. (2001). "Out-of-Plane Fatigue Cracking in Welded Steel Bridges: Why it happened and how it will be reapired." *Weld. Inovation*, 18(2), 2–7.

Roy, M., Lang, C., and May, I. (2009). "Modelling composite repairs to cracked metal structures." *Proc., Institution of Civil Engineers (ICE)-Structures and Buildings*, 162(2), 107–113.

Sabelkin, V., Mall, S., and Avram, J. B. (2006). "Fatigue crack growth analysis of stiffened cracked panel repaired with bonded composite patch." *Eng. Fract. Mech.*, 73(11), 1553–1567.

Schubbe, J. J., and Mall, S. (1999a). "Modeling of cracked thick metallic structure with bonded composite patch repair using three-layer technique." *Compos. Struct.*, 45(3), 185–193.

Schubbe, J. J., and Mall, S. (1999b). "Investigation of a cracked thick aluminum panel repaired with a bonded composite patch." *Eng. Fract. Mech.*, 63(3), 305–323.

Tavakkolizadeh, M., and Saadatmanesh, H. (2003). "Fatigue strength of steel girders strengthened with carbon fiber reinforced polymer patch." *J. Struct. Eng.*, 10.1061/(ASCE)0733-9445(2003)129:2(186), 186–196.

Umamaheswar, T. V. R. S., and Singh, R. (1999). "Modelling of a patch repair to a thin cracked sheet." *Eng. Fract. Mech.*, 62(2), 267–289.

Wang, Q. Y., Li, T., and Ning, J. X. (2002). "Fatigue crack growth behavior of bonded composite repairs." *Third Int. Conf. on Experimental Mechanics, Proc. of SPIE*, 4537.